

Υ -suppression by screening, gluodissociation and collisional damping at the LHC



Felix Nendzig,* Georg Wolschin

Institut für Theoretische Physik, Universität Heidelberg, Germany, EU

* f.nendzig@thphys.uni-heidelberg.de



1. Introduction

The suppression of quarkonium ($Q\bar{Q}$) states is one of the most promising probes for the properties of the quark-gluon plasma (QGP) that is generated in heavy-ion collisions at highly relativistic energies. In the QGP the confining potential is screened due to the interaction of the heavy $Q\bar{Q}$ with medium partons and hence, charmonium and bottomonium states successively melt [1] at sufficiently high temperatures T_{diss} beyond the critical value $T_c \approx 170$ MeV. However, additional processes such as gluon-induced dissociation, and collisional damping contribute to the suppression. Here we concentrate on such processes.

Charmonium suppression has been studied since 1986 in great detail both theoretically, and experimentally at energies reached at the CERN SPS, BNL RHIC [2, 3, 4, 5], and CERN LHC [6, 7]. Bottomonium suppression is expected to be a cleaner probe. The $\Upsilon(1S)$ ground state with mass 9.46 GeV is strongly bound. It melts as the last $Q\bar{Q}$ in the QGP (depending on the potential) only at about 4.10 T_c [8]. Even at LHC energies the number of $b\bar{b}$ -pairs in the QGP remains small such that statistical recombination is unimportant. Υ suppression in heavy-ion collisions has recently been observed for the first time both by the STAR experiment at RHIC [9], and by the CMS experiment at LHC [10, 11]. Preliminary CMS data from the 2011 run [12] have much better statistics such that the $\Upsilon(2S)$ state can be resolved individually.

In this work we investigate the suppression of $\Upsilon(1S,2S,3S)$ states at LHC energies due to screening and gluon-induced dissociation [13], collisional damping and reduced feed-down from the $\Upsilon(2S,3S)$ and $\chi_b(1P,2P)$ states.

2. Bottomonium wave functions

Due to the small relative velocity $v \ll c$ of the quarks in the bound state, $Q\bar{Q}$ may be properly described by a Schrödinger equation, with the color-singlet potential V . We use for the short-range part of the potential the complex, coulombic expression which results from pNRQCD and the HTL approximation [16, 17], while the long range part is parameterized as in [18] so that the full potential reads

$$V(r, m_D) = \frac{\sigma}{m_D} (1 - e^{-m_D r}) - \frac{4\alpha_s^s}{3} \left(m_D + \frac{e^{-m_D r}}{r} \right) - i \frac{4\alpha_s^s}{3} T \int_0^\infty \frac{dz 2z}{(1+z^2)^2} \left(1 - \frac{\sin(m_D r z)}{m_D r z} \right), \quad (1)$$

with the Debye mass $m_D = T \sqrt{4\pi\alpha_s^h (N_c/3 + N_f/6)}$, number of colors $N_c = 3$, number of flavors in the QGP $N_f = 3$, and the strong coupling constant at the soft scale, $\alpha_s^s = \alpha_s(m_b \alpha_s) \simeq 0.37$ and hard scale $\alpha_s^h = \alpha_s(m_b) \simeq 0.24$ ($m_b = 4.77$ GeV), respectively. The imaginary part of the potential accounts for collisional damping by the plasma particles. Resulting $Q\bar{Q}$ wave functions are given in Fig. 1.

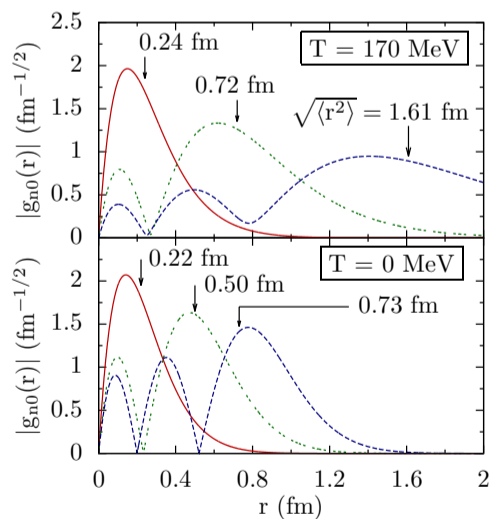


Figure 1: Radial wave functions of the $\Upsilon(1S)$, (2S), (3S) states (solid, dotted, dashed curves, respectively) calculated in the complex, screened potential (1) for temperatures $T = 0$ MeV (bottom) and 170 MeV (top) with effective coupling constant $\alpha_{\text{eff}} = (4/3)\alpha_s^s = 0.49$, and string tension $\sigma = 0.192$ GeV². The rms radii $\sqrt{\langle r^2 \rangle}$ of the 2S and, in particular, 3S state strongly dependent on temperature T , whereas the ground state remains nearly unchanged.

3. Gluodissociation and screening

Due to the high gluon density reached at LHC energies in the mid-rapidity region, gluodissociation is a major processes besides screening and collisional damping that leads to a suppression of Υ 's at LHC. Hence we calculate the gluodissociation cross sections for the 1S-3S, and 1P-2P states for different lifetimes t_{QGP} of the QGP.

The leading-order dissociation cross section of the $Q\bar{Q}$ states through E1 absorption of a single gluon had been derived by Bhanot and Peskin (BP) [19]. We have modified the approach to approximately include the confining string contribution [20], and obtain for the S-states

$$\sigma_{\text{diss}}(E_g) = \frac{2\pi^2\alpha_s^u E_g}{N_c^2} \int_0^\infty dk \delta\left(\frac{k^2}{m} + \epsilon_n - E_g\right) |\langle \psi_n | \vec{r} | \chi_k \rangle|^2, \quad (2)$$

with the singlet and octet states $|\psi\rangle$, $|\chi\rangle$ and $\alpha_s^u = \alpha_s(m_b \alpha_s^u) \simeq 0.48$.

Next we average the gluodissociation cross sections over the Bose-Einstein distribution function of gluons at temperature T , thus assuming that the medium is thermalized, although the heavy $Q\bar{Q}$ is not (see Fig.2 for the gluon distribution):

$$\Gamma_{\text{diss}} = \frac{gd}{2\pi^2} \int_0^\infty \frac{dp_g p_g^2 \sigma_{\text{diss}}}{\exp[E_g/T] - 1}. \quad (3)$$

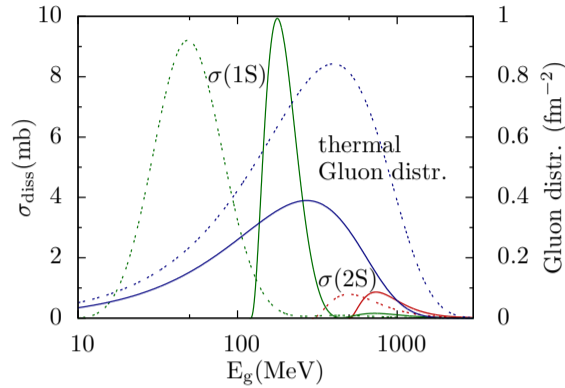


Figure 2: Gluodissociation cross sections $\sigma_{\text{diss}}(nS)$ in mb (lhs scale) of the $\Upsilon(1S)$ and $\Upsilon(2S)$ states calculated using the screened complex potential for temperatures $T = 170$ (solid curves) and 250 MeV (dotted curves) as functions of the gluon energy E_g . The thermal gluon distribution (rhs scale; solid for $T = 170$ MeV, dotted for 250 MeV) is used to obtain the thermally averaged cross sections through integrations over the gluon momenta.

4. Fireball

The density distribution of the lead ions is modeled by a Woods-Saxon potential with radius $R = 6.62$ fm and diffuseness $a = 0.546$ fm [21]. The number of produced $b\bar{b}$ -pairs at the point (x, y) in the transverse plain and impact parameter b is then proportional to the nuclear overlap T_{AA} , $N_{b\bar{b}}(b, x, y) \propto N_{\text{coll}}(b, x, y) \propto T_{AA}(b, x, y)$. The temperature is parameterized depending on the number of collisions, and on the fireball volume according to $V^{-1/4}$,

$$T(b, t, x, y) = T_c \frac{T_{AA}(b, x, y)}{T_{AA}(0, 0, 0)} \left(\frac{V(0, t_{\text{QGP}})}{V(b, t)} \right)^{-1/4}, \quad (4)$$

where t_{QGP} is the maximum lifetime of the quark-gluon plasma. The expansion velocity is set to $v_z = 0.9c$, $v_\perp = 0.6c$. The dissociation in the fireball then leads to a preliminary suppression factor

$$R_{AA}^{\text{prel}} = \frac{\int d^2b \int dx dy T_{AA}(b, x, y) e^{-\int dt \Gamma_{\text{tot}}(b, t, x, y)}}{\int d^2b \int dx dy T_{AA}(b, x, y)}. \quad (5)$$

The preliminary suppression factor R_{AA}^{prel} is displayed in Fig. 3 for the $\Upsilon(1S)$ and $\Upsilon(2S)$ states for a central ($b = 0$ fm) and a peripheral collision ($b = 10$ fm).

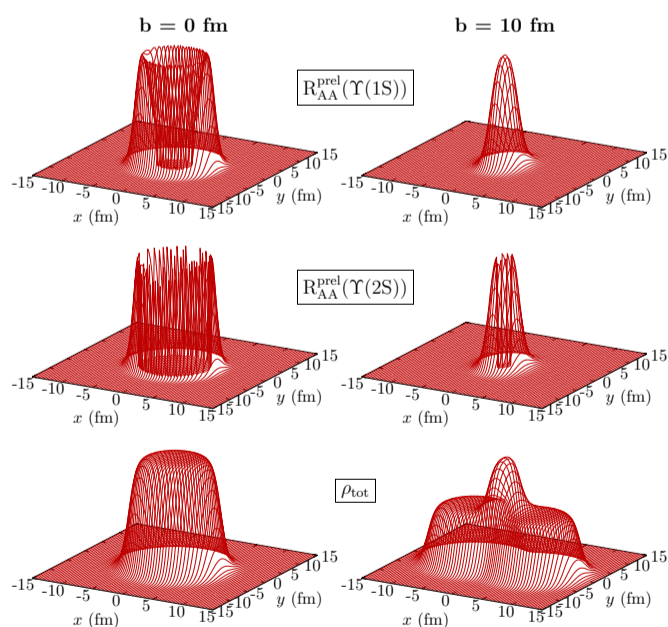


Figure 3: Scaled populations of $\Upsilon(1S)$ (top) and $\Upsilon(2S)$ (middle) after the fireball has cooled, projected on the transverse plane, for $b = 0$ fm (left) and $b = 10$ fm (right). The corresponding maximum density of both Pb-nuclei during the collision is also displayed (bottom). Clearly the $\Upsilon(2S)$ is suppressed more efficiently by the dissociation processes in the QGP. Also the stronger suppression in the central regions of the collision due to the higher temperature is obvious. The qgp lifetime is here 8 fm/c.

5. Results

Results for screening and collisional damping are derived from the solutions of the Schrödinger equation with the potential eq. (1), while the widths for gluodissociation are derived from eq. (3). The total decay widths Γ_{tot} are then inserted into a dynamic calculation for the fireball evolution. Subsequently, the bottomonium states pass through a decay cascade (see Fig. 4) so that the higher excited states feed the lower lying states. Our results for the suppression of the $\Upsilon(1S,2S)$ states in PbPb relative to pp , and of the double ratios $(2S,3S/1S)_{\text{PbPb}}/(2S,3S/1S)_{\text{pp}}$ at 2.76 TeV as functions of centrality are shown in Fig. 5, and for minimum bias in Table I.

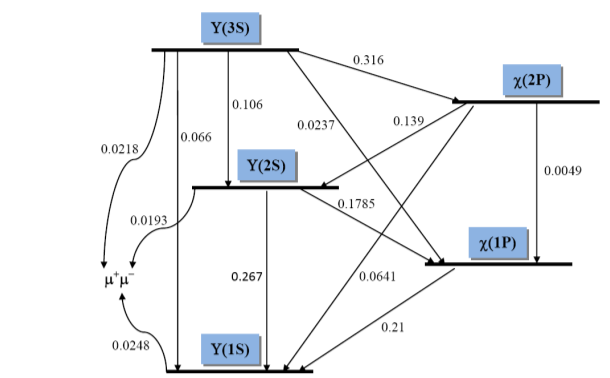


Figure 4: Branching ratios for decays within the bottomonium family $\Upsilon(nS)$ and $\chi_b(nP)$ and into dimuon pairs [22].

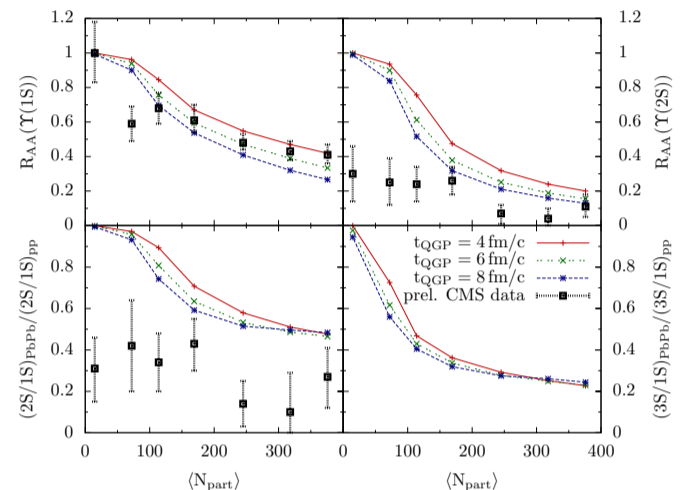


Figure 5: Suppression factors R_{AA} for the $\Upsilon(1S)$ and $\Upsilon(2S)$ states (top left and right) and the double ratios $(nS/1S)_{\text{PbPb}}/(nS/1S)_{\text{pp}}$ for $n = 2, 3$ (bottom left and right) calculated for 2.76 TeV PbPb-collisions from screening, collisional damping, gluodissociation and feed-down using three qgp lifetimes $t_{\text{QGP}} = 4, 6, 8$ fm/c for the centrality bins 0-5%, 5-10%, 10-20%, 20-30%, 30-40%, 40-50%, 50-100%. The corresponding CMS results (black) [12] are in good agreement for the $\Upsilon(1S)$ state, whereas the measured $\Upsilon(2S)$ -populations allow for additional suppression mechanisms.

	Min. Bias	Theory	Experiment
$R_{AA}(\Upsilon(1S))$		0.50	$0.56 \pm 0.08 \pm 0.07$
$R_{AA}(\Upsilon(2S))$		0.32	$0.12 \pm 0.04 \pm 0.02$
$(2S/1S)_{\text{PbPb}}/(2S/1S)_{\text{pp}}$		0.63	$0.21 \pm 0.07 \pm 0.02$
$(3S/1S)_{\text{PbPb}}/(3S/1S)_{\text{pp}}$		0.36	< 0.1

Table I: Calculated minimum bias results for $t_{\text{QGP}} = 6$ fm/c compared to the CMS results ([12], and this conference). While the $R_{AA}(\Upsilon(1S))$ is in good agreement with experiment, result for the excited states allow for additional suppression mechanisms.

6. Conclusions

Although screening of the strongly bound 1S ground state is negligible, we find that its gluodissociation is sizeable due to the strong overlap of the 1S gluodissociation cross section with the thermal gluon distribution and also collisional damping is relevant. The observed suppression factor $R_{AA}(1S) = 0.62$ in minimum-bias PbPb collisions [10] (0.53 in the preliminary 2011 data [12]) is mainly due to both direct gluodissociation and damping of the 1S state, and to the melting and gluodissociation of the excited states which partially feed the 1S state in pp , $p\bar{p}$ and e^+e^- collisions. There is, however, room for additional suppression mechanisms in particular of the excited states.

Acknowledgments

This work has been supported by the IMPRS-PTFS Heidelberg and the ExtreMe Matter Institute EMMI.



References

- [1] T. Matsui, H. Satz, Phys. Lett. B178 (1986) 416.
- [2] L. Kluberg, H. Satz, arXiv:0901.3831.
- [3] D. Kharzeev, J. Phys. G:Nucl. Part. Phys. 34 (2007) S445.
- [4] E. Atomssa, et al., Nucl.Phys.A. 830 (2009) 331c.
- [5] B. K. Patra, D. K. Srivastava, Phys. Lett. B 505 (2001) 113.
- [6] G. Martínez García, et al., J. Phys. G: Nucl. Part. Phys. 38 (2011) 124034.
- [7] C. Silvestre, et al., J. Phys. G: Nucl. Part. Phys. 38 (2011) 124033.
- [8] C.-Y. Wong, Phys.Rev.C 72 (2005) 034906.
- [9] H. Masui, et al., J. Phys. G: Nucl. Part. Phys. 38 (2011) 124002.
- [10] S. Chatrchyan, et al., Phys.Rev.Lett. 107 (2011) 052302.
- [11] S. Chatrchyan, et al., CMS-PAS-HIN-10-006.
- [12] T. Dahms, et al., Proc. Hard Probes (2012) in press.
- [13] F. Brezinski, G. Wolschin, Phys. Lett. B 707 (2012) 534.
- [14] Y. Mehtar-Tani, G. Wolschin, Phys. Rev. Lett. 102 (2009) 182301.
- [15] T. Affolder, et al., Phys.Rev.Lett. 84 (2000) 2094.
- [16] M. Laine, O. Philipsen, M. Tassler, P. Romatschke, JHEP 03 (2007) 054.
- [17] A. Beraudo, J. Blaizot, C. Ratti, Nucl. Phys. A 806 (2008) 312.
- [18] F. Karsch, M. Mehr, H. Satz, Z.Phys.C 37 (1988) 617.
- [19] G. Bhanot, M. E. Peskin, Nuclear Physics B 156 (1979) 391.
- [20] F. Nendzig, Heidelberg PhD thesis (in preparation).
- [21] H. de Vries, C. de Jager, and C. de Vries, At. Data Nucl. Data Tab. 36 (1987) 495.
- [22] K. Nakamura, and Particle Data Group, J. Phys. G 37(7), (2010) 075021.